Co-loading of Levodopa and Curcumin Using Brain-targeted Protocells for Improving the Efficacy of Parkinson's Disease

Wenkai Zhou
Institute of Medicinal Biotechnology, Chinese Academy of Medical Science & Peking Union Medical College

Chang Liu
Institute of Medicinal Biotechnology, Chinese Academy of Medical Science & Peking Union Medical College

Feifei Yu
Institute of Medicinal Biotechnology, Chinese Academy of Medical Science & Peking Union Medical College

Xia Niu
Institute of Medicinal Biotechnology, Chinese Academy of Medical Science & Peking Union Medical College

Xiaomei Wang
Institute of Medicinal Biotechnology, Chinese Academy of Medical Science & Peking Union Medical College

Guiling Li (liguiling@imb.pumc.edu.cn)
Institute of Medicinal Biotechnology, Chinese Academy of Medical Science & Peking Union Medical College

Xinru Li
Department of Pharmaceutics, School of Pharmaceutical Sciences, Peking University

Research Article

Keywords: Parkinson's disease, Levodopa, Curcumin, Brain targeting, Lactoferrin, Mesoporous silica nanoparticle, Protocells

Posted Date: January 19th, 2021

DOI: https://doi.org/10.21203/rs.3.rs-131164/v1

Abstract

Parkinson's disease (PD), one of the most common movement and neurodegenerative disorders, is challenging to treat. Levodopa is a common clinical drug for controlling the symptoms of PD, but it only replenishes the missing dopamine, can't protect dopaminergic neurons. While curcumin as a neuroprotective agent has been reported for treatment of PD. Herein, we present a novel organic-inorganic composite nanoparticle with brain targeting (lf-protocells) for co-delivery of levodopa and curcumin, and demonstrate its attractive use as a biocompatible platform for PD treatment. The nanoparticle system is comprised of a lactoferrin (lf) modified lipid bilayer (LB) containing curcumin as its outer membrane and mesoporous silica nanoparticles (MSNs) containing levodopa as its supporting inner core. Our studies illustrate that the lf-protocells have a spherical morphology, and can be used to co-load levodopa and curcumin efficiently; the combination of curcumin and levodopa alleviates the apoptosis of PD cells, decreases the expression of a-synuclein and increase the expression of tyrosine hydroxylase in SH-SY5Y cells as compared to single drug; the binary-drug loaded lf-protocells ameliorate oxidative stress and mitochondrial dysfunction as compared to combination of free drugs; lf-protocells improve significantly the distribution in brain compared with unmodified protocells; binary-drug loaded lf-protocells have better performance of motor function in mouse than unmodified protocells and combination of free drugs. In conclusion, binary-drug loaded lf-protocells show better therapeutic efficacy in both cell model and mouse model of PD than combination of free drugs and lower toxicity than bare MSNs. These results suggest that lf-protocells can be used as a promising drug delivery platform for targeted therapy against PD and other diseases of the central nervous system.

1. Introduction

Parkinson's disease (PD) is the second most common chronic progressive neurodegenerative disorder after Alzheimer's disease (AD) as it affects almost 1-2% of population aged over 65 in the world [1]. The typical pathological hallmarks of PD include the loss of dopaminergic neurons in the substantia nigra pars compacta (SNc), the decrease of tyrosine hydroxylase (TH), and the appearance of Lewy bodies formed by the accumulation of misfolded α-synuclein (α-syn) protein [2]. TH catalyzes the conversion of L-tyrosine to dihydroxyphenylalanine, which is the initial and rate-limiting step in the biosynthesis of dopamine [3].

Although the pathogenesis of PD is still unclear [4], most reports show that it is associated with oxidative stress, neuro inflammatory reaction, mitochondrial dysfunction, cell apoptosis and so on [5]. Several lines of evidence have implicated that mitochondrial dysfunction is a key element in the pathogenesis of PD [6,7]. While, oxidative stress, as a consequence of mitochondrial dysfunction, is increased in the brain tissue of patients with PD [8]. Cell apoptosis comprises two main pathways: the extrinsic pathway that does not involve mitochondria, and the mitochondrial apoptotic pathway which is involved in the pathogenesis of PD [9]. Following the inhibition of mitochondrial electron transport chain (ETC) complex I, and production of reactive oxygen species (ROS), mitochondrial apoptotic pathways can be activated [9].

Furthermore, products of PD genes are linked to apoptosis. Overexpression of wild type or mutant a-synuclein in cultured neurons also causes apoptosis [10]. A vicious cycle in which α-syn aggregation and mitochondrial dysfunction exacerbate each other could explain why these cellular changes are observed together in degenerating neurons in PD [2].

Studies have linked dysfunction of ETC complex I to PD, and many of the genes whose mutations cause familial PD are involved in mitochondrial function and homeostasis [11]. As neurotoxins, both rotenone and MPTP are the mitochondrial complex I inhibitors, which inhibit complex I and consequently increase ROS production [12]. These neurotoxins also cause neuronal death and almost completely reproduce the typical pathological and clinical features of PD, including the loss of dopaminergic neurons, the accumulation of α-syn and the mitochondrial dysfunction [12].

So far, levodopa is considered as the most effective medication for the symptomatic treatment of PD [13]. It works by being converted into dopamine and compensating for the dopamine deficiency in the brain [13]. However, the efficacy of levodopa in the late stage of PD is significantly reduced due to its metabolism, subsequent low bioavailability and irregular fluctuations of its blood concentration [14]. Extensive metabolism of levodopa, principally through decarboxylation, O-methylation, transamination and oxidation, also generate side effects such as nausea, vomiting and cardiac arrhythmias [15]. The short half-life of levodopa is a major factor responsible for fluctuating plasma levels and clinical response oscillations [16]. In general, > 95% of levodopa is metabolized in the gastrointestinal tract, liver and plasma, whereas only 1% of the ingested dose of levodopa penetrates the central nervous system (CNS) for the treatment of PD [17].

Various therapeutic strategies have been developed to extend the bioavailability of levodopa, mainly through sustained release systems, but also through the combined therapies with inhibitors of decarboxylase and O-methyltransferase [18]. However, the presence of oxidative processes in the disease has opened up new research that has led to new strategies. It is noted that several drug candidates such as EPI-743 [19], Baicalein [20] and NTCELL [21] currently used in clinical trials exert their therapeutic effects on PD by antioxidation, protecting mitochondria or acting on glial cells. It suggests that intervention of oxidative stress, improvement of mitochondrial dysfunction, resistance to neuroinflammation, protection of dopamine and other nerve cells are potential therapeutic strategies for PD [21].

As a natural polyphenol extracted from the dry rhizome of zingiberaceae plants [22], curcumin has numerous pharmacological properties such as anti-inflammation, antioxidation, anti-tumor and anti-nerve degeneration [23]. It reduces the high level of oxidative stress and neurotoxicity mainly through antioxidant effect and chelating metal ions, and thus achieves the protection of dopaminergic neurons and improves the level of dopamine [24]. Previous studies suggested that curcumin could be applied in the treatment of neurodegenerative diseases such as PD and AD [25]. Hence, if combined with levodopa, curcumin may lead to enhanced therapeutic effects of PD on the basis of levodopa supplementing neurotransmitters, since it works through antioxidation and repairing injured neurons. In other words, the

combination of these two different durgs is expected to enhance the therapeutic effect of PD. So far, no relevant pharmacological study has been reported.

However, the physicochemical properties of hydrophilic levodopa and hydrophobic curcumin are quite different, which make their co-delivery confront with great challenges. So it is necessary to construct an eligible drug delivery system that efficiently co-load these two drugs. Protocells, consisting of a mesoporous silica nanoparticles (MSNs) core coated by a layer of lipid bilayer (LB), are a class of highly scalable nanocarriers that have caused great concern in drug delivery applications [26]. Inner sponge-like inorganic MSNs with favorable surface area, high porosity and adsorption performance, extraordinary drug loading capacity, are excellent carriers of hydrophilic drugs such as levodopa. The outer membrane LB can not only contain hydrophobic drugs like curcumin but also effectively seal the surface pores of the inner MSNs to prevent drug leakage, thus achieving the co-delivery of the different drugs. In addition, these drugs can be delivered simultaneously without affecting each other.

In our study, protocells delivery system co-loaded with levodopa and curcumin were constructed, brain targeting ligand-lactoferrin (Lf) was then modified on the LB surface to enhance cellular uptake and brain targeting [27]. The blood–brain barrier (BBB) formed by brain vessel endothelial cells linked together with tight junctions, presents a major obstacle to the delivery of drugs passing from the bloodstream to the CNS [28]. Lf receptor existing on the BBB mediated endocytosis is among the most efficient cellular uptake pathway, so the delivery system modified with Lf ligand may be more efficient under certain pathological conditions of the high expression of Lf receptor, such as PD [29] and AD [30].

The physicochemical properties, efficacy *in vitro*, mechanism of action and preliminary pharmacodynamics *in vivo* of the drug delivery system named as binary-drug loaded lf-protocells (L/C-Lf-Pro) were investigated. With the modification of Lf ligand, the obstacle presented by the BBB are expected to be tackled. Moreover, L/C-Lf-Pro could offer a beneficial strategy in mitigating the adverse reaction and improving the therapeutic effect of levodopa.

2. Results

2.1 Characterization of sp-MSNs and MSNs

The DLS test indicated that the prepared MSNs had outer diameter about 90 nm, similar to the sp-MSNs without TMB modification (Tab S1). TEM images showed that the MSNs retained high monodispersity and spherical morphology, and meanwhile possessed larger porosity compared with the sp-MSNs without TMB modification (Fig. S1). According to nitrogen adsorption data, with the enlarging pores modification, the BET surface area, pore volume, and pore size were changed from 743.78 m^2/g, 1.01 cm^3/g, and 5.44 nm to 572.99 m^2/g, 1.15 cm^3/g, and 8.00 nm respectively (Fig. S2, Tab. S2).

2.2 Characterization of lf-protocells and drug loading

As for ^{1}H-NMR spectra analysis, the solvent peak of D_2O at δ 4.71 ppm was used as the reference (Fig. 1B). The ^{1}H-NMR spectrum of DSPE-PEG_{2000}-MAL clearly showed characteristic peak of MAL group at δ 6.84 ppm (Fig. 1B, top), while the disappearance of MAL peak in the ^{1}H-NMR spectrum of DSPE-PEG_{2000}-Lf (Fig. 1B, bottom) matched well with the fact that the MAL group had been reacted with the thiol group of Lf-SH. In a word, the ^{1}H-NMR spectrum demonstrated the formation of DSPE-PEG_{2000}-Lf.

The DLS test indicated that lf-protocells were larger than MSNs, up to 177 nm in diameter. The presence of the coating lipid bilayer was confirmed by TEM. As can be seen, the lf-protocells appeared to be surrounded by a ring, and the appearances of the pores were relatively vague compared with TEM image of MSNs shown in Fig. S1. The co-loading of levodopa and curcumin had little influence on the morphology of lf-protocells (Fig. 1C).

And the results of DLC and EE of various lf-protocells were shown in Tab. 1. The L-Lf-Pro yielded a levodopa DLC of 20.89 wt % (drug: MSNs) and a levodopa EE of 9.87 wt %, which were quite similar to that of binary-drug loaded lf-protocells (DLC of 21.44 wt % and EE of 10.72 wt % for levodopa). The C-Lf-Pro yielded a curcumin DLC of 1.73 wt % (drug: MSNs) and a curcumin EE of 86.67 wt %, which were also quite similar to that of binary-drug loaded lf-protocells (DLC of 1.89 wt % and EE of 88.31 wt % for curcumin). The co-loading of levodopa and curcumin showed a similar DLC and EE value to that of single-drug loaded lf-protocells, which was attributable to the possible deep immersion of levodopa in the MSNs core and the immersion of curcumin in the lipid bilayer.

In addition, the in vitro release profiles of levodopa and curcumin from binary-drug loaded lf-protocells in neutral or acidic medium were measured using HPLC (Fig. S3). Neutral medium of pH 7.4 simulated body fluid such as blood, and acidic medium of pH 5.0 simulated endosomal/lysosomal environment. The results suggested that no levodopa and only 59.2% curcumin was released from lf-protocells for 48 h in pH 7.4 solution at 37 °C. When the pH is decreased to acidic condition (pH 5.0), lf-protocells released 100% of their curcumin and 72.6% of their levodopa within 48 hours. Therefore, we speculated that the release of levodopa was hindered by the inclusion of lipid bilayer outside the inner core, which would greatly reduce its leakage in the circulatory system. However, the drug release from lf-protocells in acidic conditions is initiated by LB destabilization.

2.3 Biocompatibility and cytotoxicity of MSNs and lf-protocells

Hemolysis and cell viability assays were performed to investigate biocompatibility and cytotoxicity of MSNs (as the inner core of lf-protocells) and lf-protocells.

The hemocompatibility of MSNs, protocells and lf-protocells was evaluated by hemolysis assay at the concentrations ranging from 50 to 1000 μg/mL. The hemolytic activity of MSNs, protocells and lf-protocell on RBCs was observed using digital photography and calculated by the formula of hemolysis percentage as described in part 4.9. Visual inspection of the hemolysis experiments showed a clear color differential between samples with varying degrees of hemolysis. Uncoated MSNs showed high hemolytic

activity, roughly 40 % of the positive hemolysis control of RBCs when the concentration exceeded 400 μg/mL (Fig. S4). In contrast, with the LB coating, protocells showed the hemolytic activity below 5 % of the positive hemolysis control of RBCs, even at concentrations greater than 800 μg/mL (Fig. S4). In addition, the hemolysis ratio of lf-protocells with a concentration of 1000 μg/mL was still less than 5 % compared with the positive control group. Studies on other particle systems have determined that increasing the positive charge density of the particle leads to a decrease in hemolysis. When acidic silanols on MSNs have been masked by the lipid bilayer, no hemolysis is observed [31]. These results demonstrated that the LB coating on the surface of MSNs could reduce dramatically the hemolysis percentage, and improve markedly the biocompatibility of protocells; and modification of Lf ligand would not increase hemolytic activity.

The *in vitro* cell viability was performed by MTT assay to evaluate the toxicity of the MSNs and lf-protocells on SH-SY5Y cells. As shown in Fig. S5, over 90 % cell viability was achieved after incubating SH-SY5Y cells with 200 μg/mL of MSNs and lf-protocells respectively for 24 h, while over 85 % cell viability was achieved after incubating SH-SY5Y cells with 500 μg/mL of particles for 24 h.

2.4 Cytotoxicity of curcumin, levodopa and rotenone alone on SH-SY5Y cells

The cytotoxicity of curcumin alone, levodopa alone and rotenone alone to SH-SY5Y cells was evaluated. Cells were treated with various concentrations of curcumin (1, 2, 4 μM), levodopa (20, 40 μM) and rotenone (1, 2, 4, 10, 20 μM) respectively for 24 h, and the cell viability was determined by MTT assay. As shown in Fig. 2 C-D, curcumin alone below 4 μM did not affect cell viability, while levodopa alone did not affect cell viability at the concentrations of 40 μM or lower.

Fig. 2A showed the effect of rotenone on SH-SY5Y cell morphology. Normal SH-SY5Y cells were spindle or polygonal and had mesh connection with circumambient cells. After 24 h treatment, with the increase of concentration, rotenone induced marked cell shrinkage, disappeared connections and even loss of whole cells. The above observations indicated that rotenone created the PD cell model successfully and had obvious toxic effect on cellular morphology. As previously reported [32], a significant reduction of rotenone-induced cell viability could be observed. Our result of cytotoxicity of rotenone revealed that 1-20 μM of rotenone caused approximately 50 % of cell death after 24 h treatment (Fig. 2B). Moreover, high concentration up to 4 μM of rotenone also induced significant changes in cell morphology (Fig. 2A).

To further investigate the effects of rotenone inductionred4 on SH-SY5Y cells, western blot analysis on several important apoptosis mediated signaling pathway proteins was performed. The expression levels of pro-apoptotic factors poly ADP-ribose polymerase (PARP), Caspase-3, Cleaved Caspase-3, Bax and anti-apoptotic factors Bcl-2 were detected in 1-20 μM Rot-induced SH-SY5Y cells after 24 h cultivation. Compared with blank group, rotenone significantly increased PARP, Cleaved Caspase-3 and Bax levels and cut down Caspase-3 and Bcl-2 levels, which indicated promotion effect on apoptosis in a dose-dependent manner (Fig. S6A).

Since the typical pathological changes of PD include the deformation of dopaminergic neurons, the aggregation of intracellular α-syn protein and the decrease of TH expression, we measured the expression of α-syn and TH in Rot-induced SH-SY5Y cells. The results of western blot on TH and α-syn, shown in Fig. S6B, demonstrated that rotenone, compared with blank group, significantly decreased the level of TH and increased the level of α-syn in a dose-dependent manner.

2.5 Protection of curcumin and levodopa against rotenone-induced cytotoxicity

The cytoprotective effect of curcumin or levodopa against rotenone-induced SH-SY5Y cytotoxicity was determined by pre-treating cells with different concentrations of curcumin or levodopa for 60 min prior to rotenone exposure. Pretreatment with curcumin alone at 1, 2, 4 μM for 60 min prior to rotenone exposure significantly increased the cell viability to 79.2 ± 4.4, 82.6 ± 5.6, 76.9 ± 4.4% of control, respectively (Fig. 2C), and pretreatment with levodopa alone at 20, 40 μM for 60 min prior to rotenone exposure also enhanced the cell viability to 80.2 ± 4.5, 81.0 ± 4.7% of control, respectively (Fig. 2D). While co-pretreatment of 2 μM curcumin with 20 μM or 40 μM levodopa exerted dramatic raising cell viability compared with single drug treatment ((Fig. 2E, F). Therefore, 2 μM curcumin and 40 μM levodopa were chosen for the subsequent experiments. The concentration of levodopa and curcumin loaded in C-Lf-Pro, L-Lf-Pro or L/C-Lf-Pro were equivalent to corresponding free drug, respectively.

2.6 Lf-protocells treatment ameliorated oxidative stress in SH-SY5Y cells induced by rotenone

2.6.1 Lf-protocells protected against rotenone-induced ROS production.

The levels of ROS were determined by the intensity of DCF fluorescence within cells. As shown in Fig. 3A, exposure of rotenone (4 μM) led to a dramatic increase of DCF fluorescence intensity in SH-SY5Y cells compared with that in control group. After the pretreatment of single drug alone, neither curcumin nor levodopa, could decrease the high level of intracellular ROS induced by rotenone. However, co-treatment of curcumin and levodopa (free L/C), as well as treatment of L/C-Lf-Pro, significantly decreased rotenone-induced ROS production ($P < 0.05$, $P < 0.001$, respectively). Interestingly, treatment with L/C-Lf-Pro markedly scavenged rotenone-induced ROS compared with free L/C group ($P < 0.05$), L group ($P < 0.001$), and C group ($P < 0.001$), respectively. In brief, our study showed that L/C-lf-protocells exerted significant effect on reduction of intracellular ROS level in SH-SY5Y cells activated by rotenone.

2.6.2 Lf-protocells improved the SOD activity.

Superoxide dismutase (SOD), as an anti-oxidative defense enzyme, plays a crucial role in maintaining cellular redox homeostasis [33]. Thus, we determined the effect of lf-protocells on the enzyme activities of SOD. As shown in Fig. 3B, rotenone (4 μM) significantly decreased the SOD activity in SH-SY5Y cells ($P < 0.01$). Oxidative stress induced by rotenone was confirmed by the reduced expression of SOD. While curcumin & levodopa co-treatment in the form of free drugs (free L/C) and lf-protocells (L/C-Lf-Pro) significantly improved the enzyme activities of SOD reduced by rotenone ($P < 0.01$), and both of them were superior to single free drug treatment ($P < 0.05$). In addition, pretreatment with L/C-Lf-Pro increased

the activity of SOD to 93.5 %, the highest among all groups, even though there was no statistical difference compared with free L/C group. In short, our study indicated that L/C-Lf-Pro could efficiently recover the SOD activity impaired by rotenone.

2.6.3 Lf-protocells improved rotenone-induced GSH depletion.

GSH is a tripeptide nonprotein anti-oxidant and redox regulator in brain in which GSH depletion probably occurs via oxidative damages caused by increased ROS with significant mitochondrial damage [34]. Based on GSH neutralizing free radicals and reactive oxygen compounds in cells, the assessment of intracellular GSH content should be thought about in further exploration. Since L/C-lf-protocells exhibited a profound effect on scavenging Rot-induced intracellular ROS and ameliorating SOD activity, we speculated that L/C-lf-protocells could also improve Rot-induced GSH depletion in SH-SY5Y cells.

As shown in Fig. 3C, the content of total GSH decreased remarkably after incubation with rotenone (4 μM) compared with control group, whereas the total GSH content increased after the co-treatment of curcumin and levodopa (free L/C), as well as treatment of L/C-Lf-Pro. Noticeably, pretreatment with L/C-Lf-Pro attenuated Rot-induced total GSH depletion, the best among all groups, even though there was no statistical difference compared with free L/C group. These observations implied that L/C-Lf-Pro might provide protection against Rot-induced oxidative damage in SH-SY5Y cells via regulating GSH antioxidant system to cope with oxidative stress.

The occurrence and development of PD are closely related to oxidative stress, which are involved in the process of neuronal deformation in PD. The anti-oxidative therapeutic efficacy of binary-drug loaded lf-protocells were apparently confirmed by SOD and GSH experiment *in vitro*. The results of SOD and GSH were in conformity with the ROS assay. These findings suggested that levodopa and curcumin co-loaded lf-protocells, a novel nanoparticle platform comprised of a Lf-modified LB containing curcumin as its outer membrane and MSNs containing levodopa as its supporting inner core, compared with free levodopa and curcumin, could effectively enhance the level of total GSH and SOD in damaged cells, reduce the oxidative damage, and thus protect cells against oxidative stress, improve the anti-oxidative therapeutic effect for PD.

2.7 Lf-protocells suppressed rotenone-induced reduction of the MMP

As the most important organelle, mitochondria plays a key role not only in supplying metabolic energy to cells in the form of ATP via directly participating in a number of metabolic reaction, but also in regulating the signal transmission during the apoptosis of cells [35]. The burst of ROS and depletion of intracellular SOD and total GSH can induce the drop of MMP. The collapse of MMP, in turn, can also stimulate ROS generating excessively and the level of SOD and total GSH declining [33]. Since L/C-lf-protocells exhibited a profound effect in ameliorating oxidative stress in SH-SY5Y cells induced by rotenone, we postulated that L/C-lf-protocells could also ameliorate Rot-induced oxidative damage to membrane and mitochondrial dysfunction.

As described in part 4.12, the Rh123 fluorescence intensity was used to evaluate the MMP changes in cells. As shown in Fig. 4A, the Rh123 fluorescence intensity of rotenone group was about half of that of control group, a remarkable decrease of fluorescence intensity was observed after treatment with rotenone ($P < 0.001$). Pretreatment with free drugs (including L group, C group and free L/C group), attenuated the Rot-induced mitochondrial dysfunction as reflected by increasing the fluorescence intensity of rotenone group ($P < 0.05$). In addition, pretreatment with L/C-Lf-Pro increased the fluorescence intensity significantly compared with that of free L/C group ($P < 0.05$).

Furtherly, the change of Rh123 fluorescence intensity can be displayed by a visual way with the help of fluorescent confocal microscope (Fig. 4B). The green light intensity characterizing mitochondrial function weakened owing to the addition of rotenone, followed by becoming stronger after treatment with free L/C or L/C-Lf-Pro, which were in accordance with the former results.

Since MMP reduction could induce apoptotic signalling downstream involving cytochrome C release from mitochondria and subsequent caspase activation, and could also induce proinflammatory signaling during apoptosis [36], L/C-Lf-Pro which suppressed the reduction of MMP might reduce apoptosis. As a consequence, L/C-Lf-Pro were expected to provide protection against Rot-induced oxidative damage and mitochondrial dysfunction in SH-SY5Y cells.

2.8 Lf-protocells inhibited rotenone-induced neuronal apoptosis.

To investigate the detailed mechanisms, western blot analysis on several important apoptosis mediated signaling pathway proteins was performed. Anti-apoptotic protein Bcl-2 and pro-apoptotic protein Bax play key roles in the process of apoptosis [37]. The Bcl-2 protein could block apoptotic-like forms of death [38]. While protein Bax is the key component of apoptosis caused by mitochondrial stress and increase of membrane permeability after apoptosis stimulation [37]. In addition, once the mitochondrial membrane permeability suffers from damage, Bax may be released from the intermembrane space to initiate caspase activation in the cytosol [39]. Protein Caspase-3 has a vital role to play executor of apoptosis and could crack PARP [40]. The proenzyme form of Caspase-3 is hydrolyzed and activated to a Cleaved Caspase-3 (17 kd subunit + 19 kd subunit) [41]. Moreover, PARP is one of the main shearing targets of Caspase-3 *in vivo* and could be used as a marker of apoptosis [40].

Our results, as shown in Fig. 5A, indicated that Bcl-2 and Caspase-3 were up-regulated in both free L/C group and L/C-Lf-Pro group compared with Rot group and single drug groups. Similarly, the expression of Bax, Cleaved Caspase-3 and PARP were down-regulated in both free L/C group and L/C-Lf-Pro group compared with Rot group, and the degree of decrease was markedly enhanced in binary-drug groups compared with single-drug groups. Based on the role of apoptosis mediated signaling pathway proteins as described above, these results suggested that combination of levodopa and curcumin might partially reverse the apoptosis of cells by reducing mitochondrial damage.

Since the typical pathological changes of PD include deformation of dopaminergic neurons, aggregation of intracellular α-syn protein and decrease of TH expression, we measured the expression of these PD related proteins using certain experiments.

The results of western blot on TH and α-syn showed that rotenone could significantly decrease the level of TH and increase the level of α-syn compared with Control group, while levodopa and curcumin reversed this trend (Fig. 5B). The addition of both free L/C and L/C-Lf-Pro increased TH level and decreased α-syn level. Interestingly, the performance of binary-drug group was better than single-drug group. Since TH is the key enzyme in dopamine synthesis, co-delivery of levodopa and curcumin is expected to promote the dopamine synthesis by increasing TH expression. Moreover, the addition of levodopa as a dopaminergic neurotransmitter supplement would further increase dopamine levels. Therefore, the results demonstrated that levodopa and curcumin could protect dopaminergic neurons through decreasing the aggregation of α-syn protein and increasing the activity of TH.

Overall, these studies implied that L/C-Lf-Pro pretreatment may alleviate the apoptosis of PD cells and protect dopamine neurons through the following mechanisms: reducing the accumulation of unfolded or misfolded α-syn proteins, enhancing the level of TH and transforming more levodopa into dopamine for supplementing the loss of dopamine in the brain, reducing the mitochondrial damage and dysfunction, down-regulating the expression of Bax protein and up-regulating the expression of Bcl-2, inhibiting the activation of Caspase-3 and thus exerting an anti-apoptotic ability, showing a protective effect in the degenerative changes of dopamine neurons finally.

2.9 Cellular Uptake

The bEnd.3 cells are the brain microvascular endothelial cells in the BBB. The BBB blocks passage of most drugs. In our study, Lf-modified protocells were expected to allow more drugs to pass through BBB by the specific receptor-mediated transport. RBITC was labeled on the inner core of protocells by chemical bond, indicating the location of protocells. Calcein was loaded in protocells by the adsorption of MSNs, indicating the location of loading drugs. The cellular uptake of protocells and their loading drugs was investigated, through labeling with RBITC and Calcein respectively.

The results of cellular uptake were shown in Fig. S7. Only the blue nucleus stained with DAPI were visible in the protocells group, and no other fluorescence was seen. While the lf-protocells group showed distinct red and green fluorescence besides blue. The experimental results indicated that RBITC/Calcein-protocells were hardly internalized by bEnd.3 cells, while the modification of Lf ligand was beneficial to increase the cellular uptake of protocells and their loading drugs.

2.10 *In Vivo* Research

2.10.1 Biodistribution

Biodistribution of carrier after intraperitoneal injection of Cy5-labeled lf-protocells, unmodified protocells and bare MSNs (denoted as Cy5-lf-protocells, Cy5-protocells, Cy5-MSNs, respectively) were qualitatively

assessed by luminescence imaging *in vivo* (Fig. 6A). The results indicated that the injection site (above the right leg of mice) showed strong fluorescence intensity in all experimental groups after injection for 30 min. After 60 min, the fluorescence intensity of lf-protocells group enhanced significantly in the brain. Interestingly, the brain fluorescence intensity of lf-protocells was further increased, which was much higher than that of bare MSNs and unmodified protocells groups for 120 min. The fluorescence of bare MSNs and unmodified protocells groups concentrated mainly in abdominal cavity, with little or no enrichment in the brain during the whole time of the test.

According to these results, lf-protocells showed specific brain-targeting properties in mice, and may be distributed in the brain at a high concentration due to the modification of active targeting Lf ligand. While either bare MSNs or unmodified protocells had no brain targeting. Noteworthily, Lf is a type of ligand with brain-targeting potential, meanwhile, previous studies have demonstrated that the expression of Lf receptor was increased in the brain of PD patients [42]. Hence, the high expression of Lf receptor in cerebral microvascular endothelial cells can be utilized to achieve internalization through blood-brain barrier (BBB) by receptor-mediated transport pathway, so as to promote the brain targeting ability of lf-protocells and make them more enriched in the brain of PD patients [43]. A significant challenge of nanoparticles for targeting specific disease sites is the fact that most nanoparticles become trapped in the liver [44]. Recent study showed that different shaped MSNs were mainly trapped in reticuloendothelial system of the liver, spleen, and lung, accounting for over 80% of the injected dose at 2 h after administration [45]. Obviously, with the coating of Lf modified membrane, lf-protocells partly avoided being trapped by the reticuloendothelial system and more enriched into the brain.

2.10.2 L/C-Lf-Pro ameliorated motor function deficits in MPTP-induced PD model mice.

Animal models of Parkinson's disease (PD) have been widely used in the past four decades to investigate the pathogenesis and pathophysiology of this neurodegenerative disorder. Classical models based on the systemic or local administration of neurotoxins, like MPTP, are able to replicate most of the pathological and phenotypic features of PD in mammals [46]. Exposure to MPTP induces a PD-like syndrome such as motor retardation in mice [47]. In the brain, MPTP is converted to MPP^+, which is selectively transported into dopaminergic neuron axon terminals, causing oxidative stress, mitochondrial dysfunction, and cell death [48].

In our study, the motor function of PD mice induced by MPTP was assessed using the open-field test. The results indicated that motor function of PD mice was significantly attenuated from day 1 to day 5 in the MPTP group, compared with the control group ($P < 0.001$). Neither levodopa nor levodopa/curcumin did affect the improvement of motor function; however, L/C-Pro and L/C-Lf-Pro significantly rescued the reduction of motor function induced by MPTP ($P < 0.05$, $P < 0.01$, respectively) (Fig. 6B), and the improvement effect of L/C-Lf-Pro was superior to that of L/C-Pro ($P < 0.05$).

These results suggested that levodopa and curcumin co-loaded lf-protocells had better therapeutic effect on PD-related motor deficits than other groups. One of the possible reasons is that lf-protocells can

package drugs into nanoparticles for elevating the bioavailability of drugs. Especially, lf-protocells have an active brain-targeting distribution, which can deliver more drugs into the brain and exploit the advantages to treat PD. But it is important to note that the behavioral judgement of autonomic activity in mice includes a variety of evaluation systems, one of which is selected in our experiment. Meanwhile, behavioral evaluation is only a part of PD efficacy at the animal level. Therefore, the PD therapy evaluation of lf-protocells needs to be further completed at the animal level in our study.

3. Discussion And Conclusion

In summary, this work prepared and characterized organic-inorganic composite nanoparticles (namely lf-protocells) which were formed by coating MSNs with lf-modified lipid bilayer for levodopa/curcumin co-delivery to brain, evaluated therapeutic effects of the binary-drug loaded lf-protocells on PD both *in vitro* and *in v*ivo, and explored the possible related mechanism (Fig. 7).

Firstly, we successfully synthesized a single carrier named lf-protocells to co-deliver levodopa and curcumin at an optimized drug ratio passing through the BBB for the treatment of PD. Various physicochemical characteristics of MSNs and lf-protocells have been elucidated. Protocells, which are formed by the encapsulation of MSNs cores within supported LB, have the advantages of both liposomes and MSNs: drugs with different properties, such as levodopa and curcumin, could be loaded in different positions of the carrier; the adhesion energy between the MSNs and LB suppresses large-scale membrane bilayer fluctuations responsible for liposome instability and leakage, while the LB serves to retain water-soluble cargos within the MSNs [49]. Further safety evaluation in our study indicated that lf-protocells possessed high biocompatibility and low cytotoxicity. The biodegradation behaviors of MSNs have been concerned recently. Researchers [50] proved that MSNs exhibited the three-stage degradation behavior and finally maintained the slow degradation on day-scale. For the brain-targeted application，Jun [51] indicated that the concentration of Si in the brain was decreased after injection for up to 7 days, by which time the level had decreased by nearly 92.4%. Afterwards, MSNs can be excreted mainly through renal routes containing either nanoparticles or degraded products [50].

Several different types of natural products that have been identified as potential antioxidants compounds seem to be promising tools with therapeutic potential in oxidative stress-mediated diseases including PD [52]. As a mitochondrial protective antioxidant, curcumin was typically effective for PD treatment [53]. In our study, when combined with levodopa, curcumin enhanced the protective effect on the rotenone-induced SH-SY5Y cell model of PD. Loaded in the inner core of brain-targeted lf-protocells, levodopa avoided releasing in the neutral medium of pH 7.4 simulated body fluid until it was transported into the endosome with acidic condition. Furthermore, with the modification of Lf ligand, more uptake of lf-protocells allowed more dose of levodopa to enter the brain, thereby increasing the bioavailability of levodopa. It was worth noting that levodopa not only acted as a dopamine precursor, but also showed a certain degree of anti-oxidative activity. It was reported that levodopa oxidation products prevented H_2O_2-induced oxidative damage to cellular DNA in cultured tissue cells [54].

Compared to that observed following treatment with free levodopa and curcumin, binary-drug loaded lf-protocells (L/C-Lf-Pro) could increase the distribution of drugs in the brain, thereby exhibit better effects on reducing the level of ROS, increasing the level of SOD and total GSH, ameliorating MMP reduction and decreasing the damage of oxidative stress to PD cells. Furthermore, L/C-Lf-Pro treatment not only reduced α-syn accumulation which could cause the formation of Lewy bodies, but also elevated the activity of TH which is the rate limiting enzyme for the synthesis of dopamine. Presumably, L/C-Lf-Pro not only convert more levodopa into dopamine to make up for the loss in the brain, but also inhibit MMP reduction, turn off apoptosis signaling pathway, alleviate dopaminergic neuron damage and restore cell survival rate, subsequently ameliorate the motor function deficits, since the loss of dopaminergic neurons leading to striatal dopamine depletion is the core mechanism underlying the cardinal motor features of PD [2].

In vivo, the intraperitoneal injection of L/C-Lf-Pro resulted in improvement of motor function deficits, which was evidently superior to those of any other groups. However, more experiments are required to testify the current point of view. For example, an *in vivo* study using MPTP-induced animal models is necessary to be further completed.

Overall, L/C-Lf-Pro not only replenished the loss of dopamine in the brain, but also played the neuroprotective role of antioxidant and repairing injured neurons. The synergy of two different mechanisms can yield a better efficacy for PD, which has been successfully confirmed *in vitro* and *in vivo*. Therefore, L/C-Lf-Pro have the potential to provide a new approach for the development of drug delivery system with high-efficiency and important application prospect for curing PD. As far as we know, it is the first time that combination therapy of levodopa & curcumin loaded lf-protocells has been applied in PD.

Our work also offered a basis for lf-protocells as a novel nanocarrier to the CNS. The most intriguing thing is the potential application of this approach to other CNS diseases where future lf-protocells could be extended to nanoparticle delivery system for a broad range of drugs, genes or cell-specific targeting.

4. Methods

4.1 Materials

Tetraethyl orthosilicate (TEOS, 98%), cetyltrimethylammonium bromide (CTAB, > 99%), Brij-58 and 2-iminothiolane hydrochloride (Traut's reagent) were purchased from Aladdin-chemistry (Shanghai, China). Lactoferrin was obtained from China Peptides Co. (Shanghai, China). 1,3,5-trimethylbenzene (TMB) and curcumin were purchased from Alfa Aesar (Shanghai, China). 3-(4,5-Dimethylthiazol-2-yl)-2,5-diphenyltetrazolium bromide (MTT) and rhodamine 123 (Rh123) were purchased from Sigma Aldrich (USA). Cy5-SE was from MedChemExpress (USA). Triton X-100 was from Beijing Innochem Science & Technology Co., Ltd (Beijing, China). Total Superoxide Dismutase Assay Kit with WST-8, GSH and GSSG Assay Kit, primary antibody dilution buffer, transfer buffer and BeyoECL Moon were purchased from

Beyotime Institute of Biotechnology (Shanghai, China). DMEM/F-12 medium, fetal bovine serum (FBS), penicillin-streptomycin and phosphate buffer saline (PBS) were purchased from Corning (USA). 1,2-distearoyl-*sn*-glycero-3-phosphoethanolamine-N- [methoxy(polyethylene glycol)-2000] (DSPE-PEG_{2000}), 1,2-distearoyl-*sn*-glycero-3- phosphoethanolamine-N-[maleimide(polyethylene glycol)-2000] (DSPE-PEG_{2000}- MAL), dipalmitoyl phosphatidylcholine (DPPC) and cholesterol (Chol) were purchased from A.V.T. Pharmaceutical Co., Ltd (Shanghai, China). Rotenone (Rot), 1-methyl-4-phenyl-1,2,3,6-tetrahydropyridine (MPTP), borate-EDTA buffer, Rhodamine B isothiocyanate (RBITC), (3-Aminopropyl) triethoxysilane (APTES) and SDS-PAGE running buffer were purchased from Dalian Meilun Biotechnology Co., Ltd (Dalian, China). Levodopa (>98%) was purchased from Beijing Innochem Science & Technology Co., Ltd (Beijing, China). DAPI, Reactive Oxygen Species Assay Kit, BCA Protein Assay Kit, RIPA buffer, SDS-PAGE Gel Kit, loading buffer (with DTT, 4X) and Color Mixed Protein Marker were obtained from Beijing Solarbio Science & Technology Co., Ltd (Beijing, China). Anti-β-actin, anti-GAPDH, anti-α-synuclein and anti-tyrosine hydroxylase (TH) antibodies were obtained from Proteintech, USA. Anti-Bcl-2, anti-Bax, anti-Caspase-3 and anti-PARP antibodies were received from Cell Signaling Technology, USA. Secondary antibodies HRP-conjugated Affinipure Goat Anti-Mouse IgG(H+L) and Anti-Rabbit IgG(H+L) were obtained from Proteintech, USA. Deionized water was used in all experiments and analyses. All other chemicals were reagent grade and used directly without further purification or modification.

4.2 Cell culture and treatments

SH-SY5Y cells (purchased from the Ke Lei Biological Technology Co., Ltd.) were maintained in DMEM/F-12 medium containing 10% fetal bovine serum (FBS), 1% antibiotic cocktail of penicillin-streptomycin at 37 °C under an atmosphere of 5 % CO_2 and 90 % relative humidity.

The SH-SY5Y cells were subsequently divided into 8 experimental groups: (1) the control group: DMEM/F-12 medium alone, (2) the rotenone group: rotenone solution alone (Rot), (3) the curcumin group: 2 μM curcumin (C) + Rot, (4) the levodopa group: 40 μM levodopa (L) + Rot, (5) the levodopa and curcumin group: (40 μM levodopa + 2 μM curcumin) (free L/C) + Rot, (6) the curcumin-loaded lf-protocells group: 2 μM curcumin-loaded lf-protocells (C-Lf-Pro) + Rot, (7) the levodopa-loaded lf-protocells group: 40 μM levodopa-loaded lf-protocells (L-Lf-Pro) + Rot, and (8) the levodopa/curcumin co-loaded lf-protocells group: (40 μM levodopa + 2 μM curcumin)-loaded lf-protocells (L/C-Lf-Pro) + Rot. The molar concentration of levodopa and curcumin loaded in C-Lf-Pro, L-Lf-Pro or L/C-Lf-Pro group were equivalent to corresponding free drug group.

4.3 Animals

The male C57BL/6 mice (10 weeks old) and male BALB/c nude mice (initial weight of 18–20 g) provided by SPF (Beijing) Biotechnology Co., Ltd were kept under specific-pathogen-free condition. All animal experimental protocols were approved by the ethics committee of Chinese Academy of Medical Science & Peking Union Medical College (Animal protocol number: male C57BL/6 mice, IMB-20180104D8; male BALB/c nude mice, IMB-20171224D8). Mice had free access to standard chow diet and water and were

maintained in plastic cages filled with hardwood chips in a temperature-controlled room (24 ℃) on a 12:12 h light/dark cycle for 7 days prior to the experiments.

4.4 Synthesis of small pore MSN (sp-MSNs) and MSNs

Various mesoporous silica nanoparticles (MSNs) were prepared by sol-gel phase transition method according to the literature [55] with little modification. In brief, 0.437 g of CTAB and 0.472 g of Brij58 (as the structure-directing agents) were dissolved in 100 mL of 0.1 M phosphate buffer solution (pH 7.4). With vigorous stirring for 20 min at 60 ℃, 2.14 mL of TEOS (as the silica source) was added to the solution at a rate of approximately 30 drops per minute, and the stirring process at 60 ℃ was continued for another 8 h. In order to enlarge the pore size to increase adsorption, 2 mL of TMB was added after the addition of TEOS for 40 min [56]. Then, the stirring process at 60 ℃ was continued for another 8 h. To distinguish, we called the product synthesized without adding TMB as sp-MSNs, while synthesized with adding TMB as MSNs. The resulting white precipitate of sp-MSNs or MSNs was purified to remove remaining surfactant by centrifugation and washing with ethanol and water three times each. To remove the organic template, the sediment was refluxed for 24 h at 78 ℃ in acidic ethanolic solution (ethanol: hydrochloric acid (HCl) = 60:1, v/v). And the final white precipitate was purified by centrifugation and washing with ethanol for three times.

4.5 Characterization of sp-MSNs and MSNs

For measuring particle size distribution such as mean particle size as well as PDI, sp-MSNs and MSNs were diluted to an appropriate volume with distilled water and measured by the dynamic light scattering (DLS) method (Malvern Instruments, UK) at room temperature. The nitrogen adsorption/desorption analysis was performed using an adsorption analyzer (ASAP 2460, Micromeritics, USA). According to the adsorption data, the Brunauer-Emmett-Teller (BET) and Barrett-Joyner-Halenda (BJH) models were used to calculate the specific surface areas and the pore size of sp-MSNs and MSNs. Morphology of sp-MSNs and MSNs were observed via transmission electron microscopy (TEM, JEM-100CX II, JEOL, Japan).

4.6 Preparation of lf-protocells and drug loading

Refer to Huan Meng's synthetic method of protocells [57], the coating lipid bilayer consisted of a DPPC/Chol/DSPE-PEG_{2000} mixture, the molar ratio of which was 75:20:5; these three excipients were dissolved in chloroform and placed into a round-bottom flask, the resulting lipid solution was dried to a film by a rotary vacuum evaporator (RV10 digital, IKA, Germany) for 15 min at room temperature. Following the addition of 2 mL MSNs suspension to the as-prepared coating lipid film at a ratio of 1:1 (w/w dry weight), probe sonication was used for 15 min with 15/15 s on/off working cycle at a power output of 50 W. Since the resulting suspension contained protocells, liposomes and others, the protocells were separated by centrifugation at 12000 rpm for 10 min, followed by washing three times in saline.

Lf modified protocells (denoted as lf-protocells) were prepared according to a previously described method with slight modifications [27]. Lf was dissolved in borate-EDTA buffer (pH 8.0) containing Traut's

reagent for 2 h at 4℃. The obtained Lf-SH was mixed with DSPE-PEG_{2000}-MAL in PBS (pH 7.0) for 24 h under constant shaking in the dark at 4℃. Thereafter, the product was dialyzed and freeze-dried to acquire the conjugate DSPE-PEG_{2000}-Lf in powder form. The coating lipid bilayer consisted of a DPPC/Chol/DSPE-PEG_{2000}/DSPE-PEG_{2000}-Lf mixture, the molar ratio of which was 75:20:4:1. Finally, lf-protocells were obtained according to the above preparation method of protocells.

To obtain levodopa-loaded MSNs, levodopa was dissolved in HCl (pH 1.0) with a concentration of 10 mg/mL, then 10 mg of MSNs were soaked in 2 mL of the levodopa solution for 48 h under light-sealed condition at room temperature.

To obtain curcumin-loaded lipid film, 200 μg curcumin was added to the mixed lipid solution as previously described followed by rotary evaporation drying to form the lipid film containing curcumin.

To achieve co-loading of levodopa and curcumin, the levodopa-loaded MSNs suspension was added to the lipid film containing curcumin, followed by rehydration, sonication, centrifugation, and washing, similar to preparation method of protocells described above. The Fig. 1A depicted the preparation procedure for lf-protocells as a nanocarrier for co-loading of levodopa and curcumin.

4.7 Characterization of lf-protocells

The conjugate DSPE-PEG_{2000}-Lf was identified by ^{1}H-NMR spectroscopy. DSPE-PEG_{2000}-MAL and DSPE-PEG_{2000}-Lf were dissolved in D_2O respectively and analyzed in a ^{1}H-NMR spectrometer (Bruker, Switzerland).

For measuring particle size distribution such as mean particle size and PDI of various lf-protocells (unloaded and drug-loaded), nanoparticles were diluted to an appropriate volume with distilled water and measured by the DLS method (Malvern Instruments, UK) at room temperature. Unloaded and drug-loaded lf-protocells were characterized for morphology using a TEM (JEM-100CX II, JEOL, Japan). A minimum of three images for each sample was captured.

4.8 Encapsulation efficiency and drug loading content of lf-protocells

The encapsulation efficiency (EE) and drug loading content (DLC) of drug-loaded lf-protocells were determined by a subtraction method as the following equations:

$$EE(\%)=\frac{(\text{total mass of drug in loading})-(\text{the mass of non-encapsulated drug})}{\text{total mass of drug in loading}}\times 100$$

$$DLC(\%)=\frac{(\text{total mass of drug in loading})-(\text{the mass of non-encapsulated drug})}{\text{total mass of MSNs}}\times 100$$

The concentration of levodopa was determined by high-performance liquid chromatography (HPLC) with the mobile phase composed of tetrahydrofuran and 0.1 % TFA (3:97, v/v), and UV detection operated at 280 nm; while the concentration of curcumin was determined by HPLC with the mobile phase composed of methanol and 4 % acetic acid (75:25, v/v), and UV detection operated at 430 nm.

4.9 Hemolysis assay of MSNs and lf-protocells

Hemolysis assays were used to assess the safety of MSNs and lf-protocells for *in vivo* applications. After collection of beagle dog blood samples (provided by our cooperative laboratory), red blood cells (RBCs) were collected by centrifugation at 1000 rpm for 10 min. After discarding the supernatant and washing three times with sterile isotonic saline, the RBCs suspension was diluted to a concentration of 2 % (v:v). Subsequently, 0.4 mL of 2 % RBCs suspensions were mixed with 0.8 mL of MSNs (or lf-protocells) suspensions in saline at concentrations of 50, 100, 200, 400, 600, 800, and 1000 μg/mL, respectively. The hemolysis of RBCs in saline and 5 % Triton X-100 served as negative and positive control, respectively. The mixtures were incubated at 37 ℃ for 1 h and then centrifuged at 1000 rpm for 3 min. The supernatants were measured at 540 nm using a microplate reader (BioTek Synergy H1, USA). The following formula was used to calculate the hemolysis percentage:

$$\text{Hemolysis percentage (\%)} = \frac{(\text{absorbance of the sample - absorbance of the negative control})}{(\text{absorbance of the positive control - absorbance of the negative control})} \times 100$$

4.10 *In Vitro* cell viability by MTT assay

Cellular toxicity of MSNs and lf-protocells was determined by MTT assay. SH-SY5Y cells were seeded in 96-well plates (1×10^4 per well) and incubated for 24 h. Subsequently, cells were exposed to various concentrations of MSNs or lf-protocells for an additional period of 24 h, cell viability was then determined using a colorimetric assay with MTT.

To determine the toxicity of rotenone, SH-SY5Y cells were incubated with different concentrations of rotenone (0.5, 1, 2, 4, 10 and 20 μM) for 24 h, cell viability was then determined by MTT assay.

To determine the neuroprotective effects of free drugs (levodopa and curcumin) against rotenone-induced cytotoxicity, SH-SY5Y cells were cultured in 96-well plates (1×10^4 per well) for 24 h as above, and were pretreated with free drugs (the concentrations of curcumin were 1, 2, 4 μM and the concentrations of levodopa were 20, 40 μM). Then these cells were treated with 4 μM rotenone for 24 h, cell viability was determined by MTT assay.

For the MTT assay, each well was treated with 100 μl of MTT-labeling reagent (0.5 mg/mL), and the plate was incubated for an additional 3 h. The resulting formazan crystals were dissolved with 150 μl of dimethyl sulfoxide, and MTT reductions were detected at 595 nm by the microplate reader (BioTek Synergy H1, USA).

4.11 Oxidative stress detection

4.11.1 Measurement of intracellular ROS

In order to determine the cellular ROS level, Reactive Oxygen Species Assay Kit was used, in which 2', 7'-dichlorofluorescein diacetate (DCFH), a specific ROS fluorescence probe, can be oxidized into fluorescent DCF in the presence of ROS, so the level of ROS can be measured by the intensity of DCF [58]. SH-SY5Y cells (about 1×10^5 cells/well in 6-well plates) were cultured for 24 h. After treatment as described in part 4.2 above (group 1-5&8) for 24h, cells were washed twice with PBS and then incubated with 4 μM DCFH-DA in the dark for 20 min. Cells were then washed twice with PBS and harvested in trypsinization. All samples were measured via FACS calibur flow cytometer (BD, USA). Fluorescent measurements were done with excitation and emission wavelengths set at 488 nm and 525 nm, respectively. The experiment was repeated in triplicate.

4.11.2 Measurement of intracellular superoxide dismutase (SOD) activity

The SOD activity was quantified by Total Superoxide Dismutase Assay Kit with WST-8. SH-SY5Y cells were seeded in a 6-well plate at 1×10^5 cells/well and treated for 24h as described in part 4.2 above (group 1-5&8). Cells were harvested and washed twice with PBS. Then, the SOD activity of all samples was determined according to the Kit manufacturer's instructions, and the absorbance value was read at 450 nm by the microplate reader (BioTek Synergy H1, USA). The protein content was determined using the BCA protein assay. Each experiment was performed in triplicate.

4.11.3 Determination of cellular total glutathione (GSH) level

The total GSH level was quantified by GSH and GSSG Assay Kit. SH-SY5Y cells were seeded in a 6-well plate at 1×10^5 cells/well and treated as described in part 4.2 above (group 1-5&8). After 24 h incubation, cells were collected and washed twice with PBS. Then each sample was determined according to the Kit manufacturer's instructions. Then, the absorbance value was measured at 412 nm by the microplate reader (BioTek Synergy H1, USA). Each experiment was performed in triplicate.

4.12 Measurement of mitochondrial membrane potential (MMP)

To monitor the MMP changes of cultured cells, the mitochondrial specific fluorescent dye Rh123 was used. SH-SY5Y cells were seeded in 6-well plates for the treatment listed in part 4.2 above (group 1-5&8). After 24 h incubation, the medium of each sample was removed, then 1 mL FBS-free medium with 1 μM Rh123 was added, the incubation was continued for 30 min in the dark at 37 °C. Data were analyzed using a flow cytometer (BD Biosciences, USA).

To visualize the mitochondrial function of cultured cells, the medium was removed after 24 h incubation. Each sample was incubated with 1 μM Rh123 for 30 min in the dark at 37 °C. Then cells were washed twice with PBS and photographed immediately using an Ultra High Resolution Microscope (TCS SP8

STED, Leica, Germany). The results were expressed as mean Rh123 fluorescence intensity. The experiment was repeated in triplicate.

4.13 Western blot

SH-SY5Y cells treated as list in part 4.2 were lysed in RIPA lysis buffer supplemented with protease inhibitors. After quantification by BCA protein assay, samples were mixed with loading buffer (containing DTT) at a ratio of 4:1, and then boiled for 10 min. The resulting proteins were separated with SDS-PAGE and transferred onto a PVDF membrane. Then the membrane was sealed up in TBST with 5 % skim milk at room temperate for 2 h, and subsequently cultured with primary antibodies including anti-TH, anti-α-synuclein, anti-Bcl-2, anti-Bax, anti-Caspase-3, anti-PARP, anti-β-actin and anti-GAPDH at 4 °C overnight. After TBST-washing in triplicate, the membrane was incubated with secondary antibodies HRP-conjugated Affinipure Goat Anti-Mouse IgG(H+L) and Anti-Rabbit IgG(H+L) for 1 h at room temperature. Protein bands were visualized using enhanced chemiluminescence. The results were analyzed by Image J. GAPDH and β-actin were included as internal controls. The experiment was repeated in triplicate.

4.14 Cellular uptake

To investigate the uptake behavior of protocells (unmodified with Lf) and lf-protocells, fluorescence-labeled protocells and lf-protocells (denoted as RBITC/Calcein-protocells and RBITC/Calcein-lf-protocells, respectively) with RBITC-conjugated and Calcein-loaded MSNs as the inner cores were prepared.

RBITC-conjugated MSNs were prepared as follow: 8.6 mg RBITC and 200 μL APTES were dissolved in 2mL absolute ethanol. The solution reacted for 24h in the dark under stirring. CTAB, Brij58 and TEOS were added and reacted as described in part 4.4. After that, 200 μL of the above reaction solution was added. The following procedures were the same as the synthetic method of MSNs. For Calcein loading, Calcein was soaked following a similar approach of levodopa-loaded MSNs, as described above. RBITC/Calcein-protocells and RBITC/Calcein-lf-protocells were prepared refer to synthetic method of protocells as described above.

For cellular uptake assay, bEnd.3 cells were seeded on glass bottom dishes at a density of 5×10^4 cells/mL per chamber and incubated for 24 h under an atmosphere of 5 % CO_2 at 37 ℃. The cells were then treated with 200 μg/mL RBITC/Calcein-protocells or RBITC/Calcein-lf-protocells for 4 h. After washing three times with PBS, the cells were treated with 4 % paraformaldehyde for 30 min at 4 ℃ and the nucleus were subsequently labeled with DAPI. After that, the dishes were visualized under Ultra High Resolution Microscope (TCS SP8 STED, Leica, Germany). The fluorescence intensity of RBITC was determined with an excitation wavelength of 540 nm and an emission wavelength of 625 nm. The fluorescence intensity of Calcein was determined with an excitation wavelength of 496 nm and an emission wavelength of 515 nm.

4.15 *In Vivo* Study

4.15.1 ethics declarations

The authors confirm that the following animal experiments were carried out in accordance with the ARRIVE guidelines, and all methods were carried out in accordance with relevant guidelines and regulations.

4.15.2 Biodistribution

To investigate the biodistribution behavior of lf-protocells in mouse, fluorescence-labeled lf-protocells denoted as Cy5-lf-protocells were prepared using Cy5-conjugated MSNs as the inner core. For synthesis of Cy5-conjugated MSNs, 2.5 mg Cy5-SE and 200 μL APTES were dissolved in 2mL DMSO. The solution reacted for 24h in the dark under stirring. CTAB, Brij58 and TEOS were added and reacted as described in part 4.4. After that, 200 μL of the above reaction solution was added. The following procedures were the same as the synthetic method of MSNs.

The male BALB/c nude mice (n=3) were given 200 μL of 5mg/mL Cy5-lf-protocells via intraperitoneal injection, with corresponding dose of MSNs and Cy5-protocells as control. Then, the mice were anesthetized by isoflurane inhalation and scanned in an IVIS Spectrum CT system (Maestro2, CRI, USA) at various time points. The images of the mice were collected at an excitation wavelength of 649 nm and an emission wavelength of 670 nm.

4.15.3 Open-Field Test

Male C57BL/6 mice were randomly assigned to six groups (n = 5/group):

Control group were treated with saline only. PD model group were induced by MPTP, received intraperitoneal (i.p.) injections of MPTP (20 mg/kg/day) for 5 days (MPTP) [46]. Various therapeutic groups were treated with 20 mg/kg free levodopa (L), 20 mg/kg free levodopa + 2 mg/kg free curcumin (free L/C), levodopa/curcumin co-loaded protocells (L/C-Pro, encapsulated with 20 mg levodopa and 2 mg curcumin), and levodopa/curcumin co-loaded lf-protocells (L/C-Lf-Pro, encapsulated with 20 mg levodopa and 2 mg curcumin) respectively using i.p. injections at 1 h before MPTP treatment for 5 days [47]. The doses of levodopa [59] and curcumin [60] were referred to relevant studies.

To evaluate the exploratory and locomotor activities by Open-Field Test, each mouse was placed into the center of a square open-field box (24 cm * 24 cm * 10 cm, divided into sixteen squares with grids, made of transparent PVC) and acclimated for 10 min. The motor function of each mouse was evaluated by counting the number of line crossings during 5 min in the square open-field box, persist for five days [47].

4.16 Data processing

All data were presented as mean ± SD (Standard Deviation) of triplicates measurement. All statistical analysis was done in Graph Pad Prism software. Statistical differences between groups were evaluated using a two-tailed Student's t test and differences with a $P < 0.05$ were considered significant.

Abbreviations

AD	Alzheimer's disease
APTES	(3-Aminopropyl) triethoxysilane
BBB	Blood–brain barrier
C	Curcumin
Chol	Cholesterol
CNS	Central nervous system
CTAB	Cetyltrimethylammonium bromide
ETC	Electron transport chain
L	Levodopa
LB	Lipid bilayer
Lf	Lactoferrin
MPTP	1-methyl-4-phenyl-1,2,3,6-tetrahydropyridine
MSNs	Mesoporous silica nanoparticles
PD	Parkinson's disease
Pro	Protocells
RBITC	Rhodamine B isothiocyanate
Rh123	Rhodamine 123
Rot	Rotenone
sp-MSNs	Small pore mesoporous silica nanoparticles
TEOS	Tetraethyl orthosilicate
TH	Tyrosine hydroxylase
TMB	1,3,5-trimethylbenzene
α-syn	α-synuclein

Declarations

Acknowledgements

This study was supported by the CAMS Initiative for Innovative Medicine (Grant No. 2017-I2M-1-012).

Author contributions

G.L. and X.L. led the research; W.Z. and C.L. performed most of experiments and analyzed the data; F.Y., X.N. and X.W. participated in this project; C.L. and W.Z. wrote the manuscript, which G.L. and X.L. reviewed. All authors read and approved the final manuscript.

Additional information

Ethics approval and consent to participate

The study was approved by Ethics Committee of Institute of Medicinal Biotechnology, Chinese Academy of Medical Science & Peking Union Medical College (Animal protocol number: male C57BL/6 mice, IMB-20180104D8; male BALB/c nude mice, IMB-20171224D8).

Consent for publication

All authors concur with the submission and publication of this paper.

Competing interests statement

The authors declare that they have no competing interests.

Availability of data and materials

The datasets used and/or analysed during the current study are available from the corresponding author on reasonable request.

Funding

This work was supported by the CAMS Initiative for Innovative Medicine (Grant No. 2017-I2M-1-012)

References

[1] Cossu, G., Rinaldi, R. & Colosimo, C. The rise and fall of impulse control behavior disorders. *Parkinsonism & related disorders* **46 Suppl 1**, S24-S29, (2018).

[2] Poewe, W. et al, Lang, Parkinson disease. *Nat Rev Dis Primers.*. 23(3):17013. (2017).

[3] Nagatsu, T. et al, Human tyrosine hydroxylase in Parkinson's disease and in related disorders. *Journal of neural transmission*. 126, 397-409(1996).

[4] Fahn, S. The 200-year journey of Parkinson disease: Reflecting on the past and looking towards the future. *Parkinsonism & related disorders* **46 Suppl 1**, S1-S5, (2018).

[5] Calabrese, V. et al, Aging and Parkinson's Disease: Inflammaging, neuroinflammation and biological remodeling as key factors in pathogenesis. *Free radical biology & medicine.* 115, 80-91 (2018).

[6] Schapira, A. H. V. Mitochondrial dysfunction in Parkinson's disease. *Cell Death & Differentiation* **14**, 1261-1266, (2007).

[7] Bose, A. & Beal, M. F. Mitochondrial dysfunction in Parkinson's disease. *J Neurochem* **139**, 216-231, (2016).

[8] Dias, V., Junn, E. & Mouradian, M. M. The Role of Oxidative Stress in Parkinson's Disease. *Journal of Parkinson's Disease* **3**, 461-491, (2013).

[9] Bose, A., & Beal, M.F. Mitochondrial dysfunction in Parkinson's disease. *J Neurochem.* 139 Suppl 1, 216-231.(2016).

[10] Venderova, K. & Park, D.S., Programmed cell death in Parkinson's disease. Cold Spring Harbor perspectives in medicine. 2 (DOI: 10.1101/cshperspect.a009365) (2012).

[11] Hanagasi, H. A., Ayribas, D., Baysal, K. & Emre, M. Mitochondrial complex I, II/III, and IV activities in familial and sporadic Parkinson's disease. *International Journal of Neuroscience* **115(4)**, 479-493, (2005).

[12] Klingelhoefer, L. & Reichmann, H. Pathogenesis of Parkinson disease—the gut–brain axis and environmental factors. *Nature Reviews Neurology* **11(11)**, 625-636, (2015).

[13] Franco, M. R., Viana, T. F., Biscaia, S. & Bártolo, P. Levodopa Incorporation in Alginate Membranes for Drug Delivery Studies. *Advanced Materials Research* **749**, 423-428, (2013).

[14] Kestenbaum, M. & Fahn, S. Safety of IPX066 , an extended release carbidopa-levodopa formulation, for the treatment of Parkinson's disease. *Expert opinion on drug safety* **14**, 761-767, (2015).

[15] Ngwuluka, N. *et al.* Levodopa delivery systems: advancements in delivery of the gold standard. *Expert Opin Drug Deliv* **7**, 203-224, (2010).

[16] Nutt, J. G., et al. The On–Off Phenomenon in Parkinson's Disease. *New England Journal of Medicine* **310**, 483-488, (1984).

[17] Ngwuluka, N., et al. Levodopa delivery systems: advancements in delivery of the gold standard. *Expert Opin Drug Deliv*. 7, 203-224 (2010).

[18] Poewe, W. & Antonini, A. Novel formulations and modes of delivery of levodopa. *Movement Disorders* **30**, 114-120, (2015).

[19] El-Hattab, A.W., Zarante, A.M., Almannai, M., & Scaglia, F., Therapies for mitochondrial diseases and current clinical trials. *Molecular genetics and metabolism*. 122, 1-9 (2017).

[20] Li, Y., Zhao, J. & Hölscher, C. Therapeutic Potential of Baicalein in Alzheimer's Disease and Parkinson's Disease. *CNS drugs* **31**, 639-652, (2017).

[21] Xue, Z., et al, Advances in anti-Parkinson's disease drugs and their related pharmacological targets. *J Int Pharm Res..* 43, 87-96. (2016).

[22] Bollimpelli, V. S., Kumar, P., Kumari, S. & Kondapi, A. K. Neuroprotective effect of curcumin-loaded lactoferrin nano particles against rotenone induced neurotoxicity. *Neurochemistry international* **95**, 37-45, (2016).

[23] Harish, G., et al. Bioconjugates of curcumin display improved protection against glutathione depletion mediated oxidative stress in a dopaminergic neuronal cell line: Implications for Parkinson's disease. *Bioorganic & medicinal chemistry*. 18, 2631-2638 (2010).

.[24] Jagatha, B., Mythri, R.B., Vali, S., & Bharath, M.M., Curcumin treatment alleviates the effects of glutathione depletion in vitro and in vivo: therapeutic implications for Parkinson's disease explained via in silico studies. *Free radical biology & medicine*. 44, 907-917 (2008).

[25] Lee, W.H., et al. Curcumin and its derivatives: their application in neuropharmacology and neuroscience in the 21st century. *Current neuropharmacology*. 11, 338-378 (2013).

[26] Ashley, C.E., et al. The targeted delivery of multicomponent cargos to cancer cells by nanoporous particle-supported lipid bilayers. *Nature materials*. 10, 389-397 (2011).

[27] Ye, Y., et al. A novel lactoferrin-modified beta-cyclodextrin nanocarrier for brain-targeting drug delivery. *International journal of pharmaceutics.* 458, 110-117 (2013).

[28] C, B. Physiology: Double function at the blood-brain barrier. *Nature* **509**, 432-433, (2014).

[29] BA, F. *et al.* Expression of lactoferrin receptors is increased in the mesencephalon of patients with Parkinson disease. *Proceedings of the National Academy of Sciences of the United States of America* **92**, 9603-9607, (1995).

[30] Kawamata T., et al. Lactotransferrin immunocytochemistry in Alzheimer and normal human brain. *The American journal of pathology* **142**, 1574-1585, (1993).

[31] Roggers, R. A., Joglekar, M., Valenstein, J. S. & Trewyn, B. G. Mimicking red blood cell lipid membrane to enhance the hemocompatibility of large-pore mesoporous silica. *ACS applied materials & interfaces* **6**, 1675-1681, (2014).

[32] Kundu, P., Das, M., Tripathy, K. & Sahoo, S. K. Delivery of Dual Drug Loaded Lipid Based Nanoparticles across the Blood-Brain Barrier Impart Enhanced Neuroprotection in a Rotenone Induced Mouse Model of Parkinson's Disease. *ACS chemical neuroscience* **7**, 1658-1670, (2016).

[33] Chen, W., Su, H., Xu, Y. & Jin, C. In vitro gastrointestinal digestion promotes the protective effect of blackberry extract against acrylamide-induced oxidative stress. *Scientific reports* **7**, 40514, (2017).

[34] Perricone, C., De Carolis, C. & Perricone, R. Glutathione: a key player in autoimmunity. *Autoimmunity reviews* **8**, 697-701, (2009).

[35] Martinou, J.-C. & Youle, Richard J. Mitochondria in Apoptosis: Bcl-2 Family Members and Mitochondrial Dynamics. *Developmental Cell* **21**, 92-101, (2011).

[36] Bock, F. J. & Tait, S. W. G. Mitochondria as multifaceted regulators of cell death. *Nat Rev Mol Cell Biol* **21**, 85-100, (2020).

[37] Maes, M.E., Schlamp, C.L., & Nickells, R.W., BAX to basics: How the BCL2 gene family controls the death of retinal ganglion cells. *Progress in retinal and eye research.* 57, 1-25 (2017).

[38] Zheng, J.H., Viacava Follis, A., Kriwacki, R.W., & Moldoveanu, T., Discoveries and controversies in BCL-2 protein-mediated apoptosis. *FEBS J*, 283(14), 2690-2700 (2016).

[39] Skommer, J., Brittain, T. & Raychaudhuri, S. Bcl-2 inhibits apoptosis by increasing the time-to-death and intrinsic cell-to-cell variations in the mitochondrial pathway of cell death. *Apoptosis* **15**, 1223-1233, (2010).

[40] Nicholson, D.W. et al, Identification and inhibition of the ICE/CED-3 protease necessary for mammalian apoptosis. *Nature*. 376, 37-43. (1995).

[41] Taylor, R. C., Cullen, S. P. & Martin, S. J. Apoptosis: controlled demolition at the cellular level. *Nat Rev Mol Cell Biol* **9**, 231-241, (2008).

[42] Huang, R. Q. *et al.* Characterization of lactoferrin receptor in brain endothelial capillary cells and mouse brain. *Journal of biomedical science* **14**, 121-128, (2007).

[43] Fang, F. *et al.* Non-invasive approaches for drug delivery to the brain based on the receptor mediated transport. *Materials science & engineering. C, Materials for biological applications* **76**, 1316-1327, (2017).

[44] MacParland, S. A. *et al.* Phenotype Determines Nanoparticle Uptake by Human Macrophages from Liver and Blood. *ACS nano* **11**, 2428-2443, (2017).

[45] Huang, X. *et al.* The Shape Effect of Mesoporous Silica Nanoparticles on Biodistribution, Clearance, and Biocompatibility in Vivo. *ACS nano* **5**, 5390-5399, (2011).

[46] Blandini, F. & Armentero, M.-T. Animal models of Parkinson's disease. *The FEBS Journal* **279**, 1156-1166, (2012).

[47] Li, Y. *et al.* GLP-1 receptor stimulation preserves primary cortical and dopaminergic neurons in cellular and rodent models of stroke and Parkinsonism. *Proceedings of the National Academy of Sciences of the United States of America* **106**, 1285-1290, (2009).

[48] Javitch, J. A., D'Amato, R. J., Strittmatter, S. M. & Snyder, S. H. Parkinsonism-inducing neurotoxin, N-methyl-4-phenyl-1,2,3,6 -tetrahydropyridine: uptake of the metabolite N-methyl-4-phenylpyridine by dopamine neurons explains selective toxicity. *Proceedings of the National Academy of Sciences of the United States of America* **82**, 2173-2177, (1985).

[49] Butler, K. S. *et al.* Protocells: Modular Mesoporous Silica Nanoparticle-Supported Lipid Bilayers for Drug Delivery. *Small (Weinheim an der Bergstrasse, Germany)* **12**, 2173-2185, (2016).

[50] Chen, Y., Chen, H. & Shi, J. In Vivo Bio-Safety Evaluations and Diagnostic/Therapeutic Applications of Chemically Designed Mesoporous Silica Nanoparticles. *Advanced Materials* **25**, 3144-3176, (2013).

[51] Yang, J. *et al.* Rapid-releasing of HI-6 via brain-targeted mesoporous silica nanoparticles for nerve agent detoxification. *Nanoscale* **8**, 9537-9547, (2016).

[52] Huajun, J. *et al.* Mitochondria-targeted antioxidants for treatment of Parkinson's disease: preclinical and clinical outcomes. *Biochim Biophys Acta* **1842(8)**, 1282-1294, (2014).

[53] Zhohui, L., et al. Curcumin protects against A53T alpha-synuclein-induced toxicity in a PC12 inducible cell model for Parkinsonism. *Pharmacological research* **63(5)**, 439-444, (2011).

[54] Shi, Y.-l., Benzie, I. F. F. & Buswell, J. A. L-DOPA oxidation products prevent H2O2-induced oxidative damage to cellular DNA. *Life Sci* **71**, 3047-3057, (2002).

[55] Zhai, H., et al, Construction of a Glutathione-Responsive and Silica-Based Nanocomposite for Controlled Release of Chelator Dimercaptosuccinic Acid. *International journal of molecular sciences*. 19(12), E3790 (2018).

[56] Kim, M. H. *et al.* Facile synthesis of monodispersed mesoporous silica nanoparticles with ultralarge pores and their application in gene delivery. *ACS nano* **5**, 3568-3576, (2011).

[57] Meng, H. *et al.* Use of a lipid-coated mesoporous silica nanoparticle platform for synergistic gemcitabine and paclitaxel delivery to human pancreatic cancer in mice. *ACS nano* **9**, 3540-3557, (2015).

[58] Zhang, J., et al, Cell death induced by α-terthienyl via reactive oxygen species-mediated mitochondrial dysfunction and oxidative stress in the midgut of Aedes aegypti larvae. *Free Radic Biol Med*. 137, 87-98 (2019).

[59] Mytilineou, C., Walker, R.H., JnoBaptiste, R., & Olanow, C.W., Levodopa Is Toxic to Dopamine Neurons in an in Vitro but Not an in Vivo Model of Oxidative Stress. *Journal of Pharmacology and Experimental Therapeutics*. 304, 792 (2003).

[60] Wang, X.-S. *et al.* Neuroprotective properties of curcumin in toxin-base animal models of Parkinson's disease: a systematic experiment literatures review. *BMC Complement Altern Med* **17**, 412, (2017).

Table

Tab 1. Physicochemical characteristics of various Lf-Protocells (mean ± SD; n=3).

	unloaded Lf-Protocells	levodopa loaded Lf-Protocells	curcumin loaded Lf-Protocells	binary-drug loaded Lf-Protocells	
				levodopa	curcumin
Particle size(nm)	176.2 ± 1.4	226.8 ± 5.4	207.6 ± 0.8	219.3 ± 7.2	
PDI	0.176 ± 0.002	0.154 ± 0.005	0.205 ± 0.007	0.149 ± 0.005	
EE (%)	—	9.87 ± 0.38	86.67 ± 0.12	10.72 ± 0.04	88.31 ± 0.02
DLC (%)	—	20.89 ± 0.34	1.73 ± 0.02	21.44 ± 0.09	1.89± 0.01

Figures

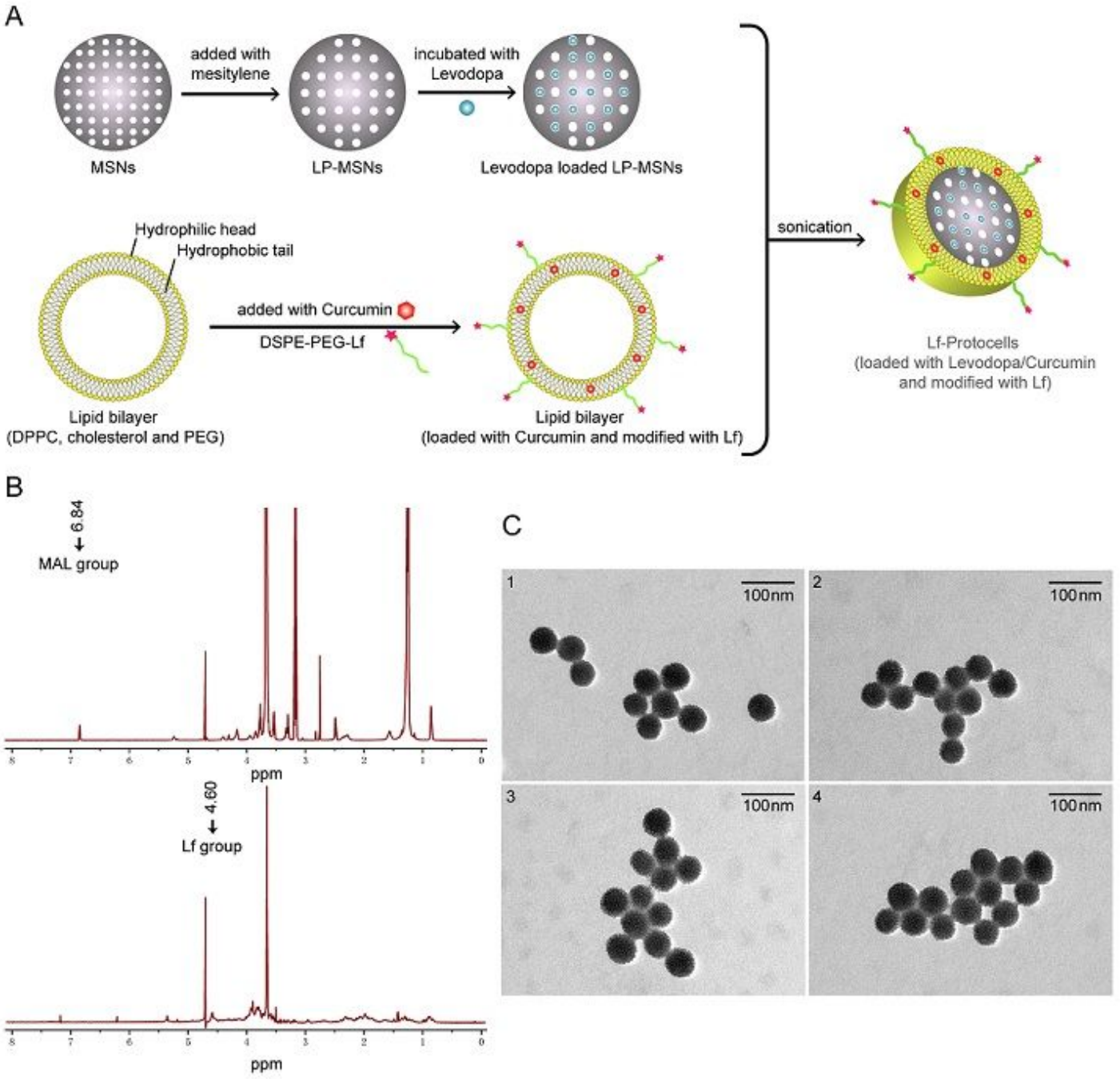

Figure 1

Preparation and characterization of lf-protocells. (A) Scheme of the preparation of lf-protocells as a carrier for co-delivery of levodopa and curcumin. (B) 1H-NMR spectra of DSPE-PEG2000-MAL (top) and DSPE-PEG2000-Lf (bottom) (D2O as the solvent). (C) TEM images of various lf-protocells. (1) unloaded lf-protocells; (2) levodopa loaded lf-protocells; (3) curcumin loaded lf-protocells; (4) binary-drug loaded lf-protocells.

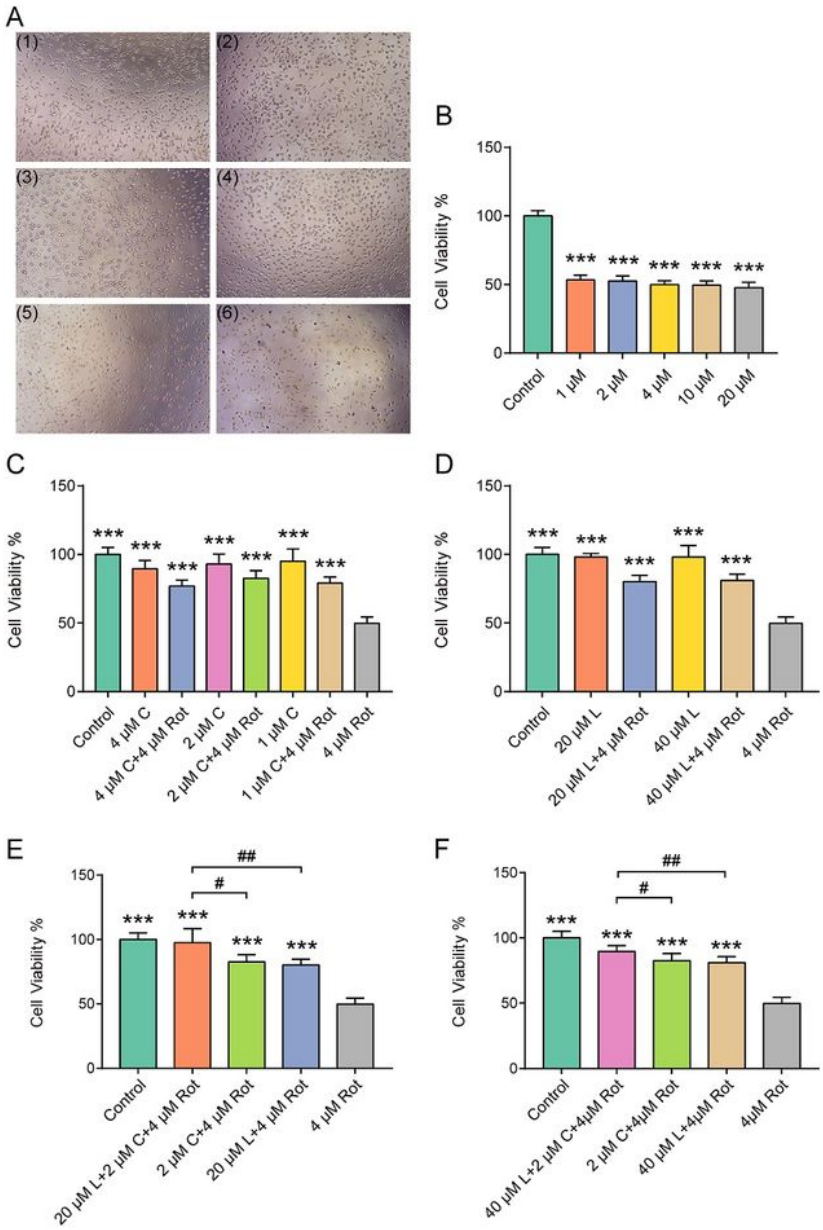

Figure 2

Effects of levodopa and curcumin on Rot-induced cytotoxicity. (A) The cellular morphology of SH-SY5Y cells induced by gradient concentration of Rot. (1) 0 μM Rot (2) 1 μM Rot (3) 2 μM Rot (4) 4 μM Rot (5) 10 μM Rot (6) 20 μM Rot; (B) Effect of gradient concentration of Rot on SH-SY5Y cells viability. (mean ± SD; n=6. *** P < 0.001 compared with the control group.) (C-D) Effects of gradient concentration of curcumin or levodopa on SH-SY5Y cells viability, as well as protection against toxicity induced by 4 μM Rot. (mean

± SD; n=6. *** P < 0.001 compared with the 4 μM Rot group.) (E-F) Protection of various combinations of gradient concentration of levodopa and curcumin against toxicity induced by 4 μM Rot. (mean ± SD; n=6. *** P < 0.001 compared with the 4 μM Rot group. # P < 0.05, ## P< 0.01 compared between two groups.) Cells were exposed for 24 h and cell viability was determined by MTT assay. Rot: rotenone; C: curcumin; L: levodopa.

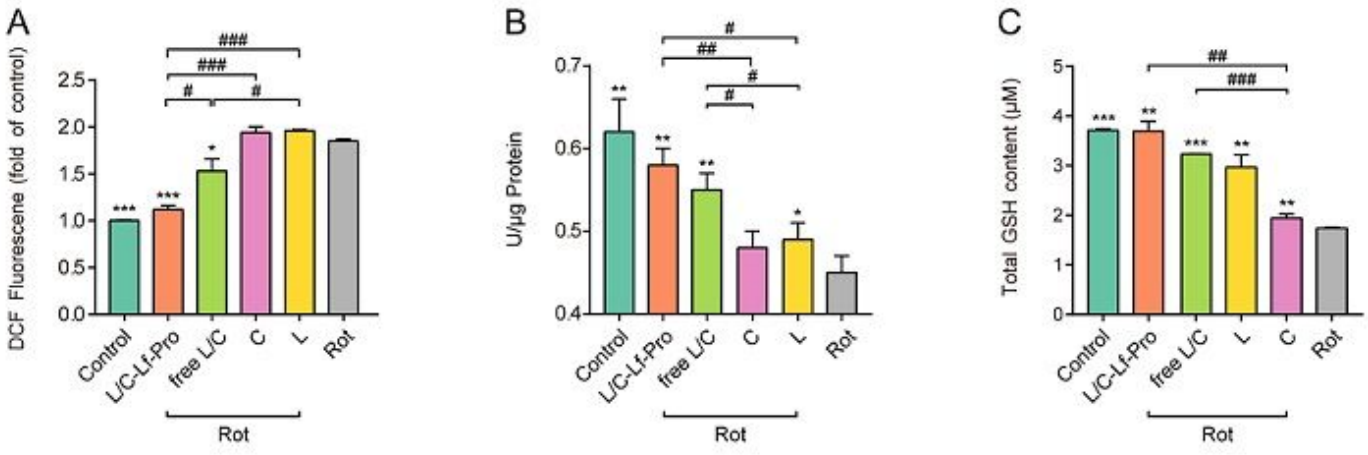

Figure 3

Lf-protocells treatment ameliorated oxidative stress in SH-SY5Y cells induced by Rot. (A) Lf-protocells protected against Rot-induced ROS in SH-SY5Y cells. The levels of intracellular ROS were quantified by DCF fluorescence intensity. The fluorescence data were obtained by flow cytometry. (B) Lf-protocells improved SOD activity reduced by Rot. SOD activity was measured and expressed as U/μg protein. (C) Lf-protocells improved Rot-induced total GSH depletion in SH-SY5Y cells. (mean ± SD, n=3. * P < 0.05, ** P < 0.01, *** P < 0.001 compared with the 4 μM Rot group. # P < 0.05, ## P < 0.01, ### P < 0.001, compared between two groups.) Rot: rotenone; C: curcumin; L: levodopa; Lf-Pro: lf-protocells.

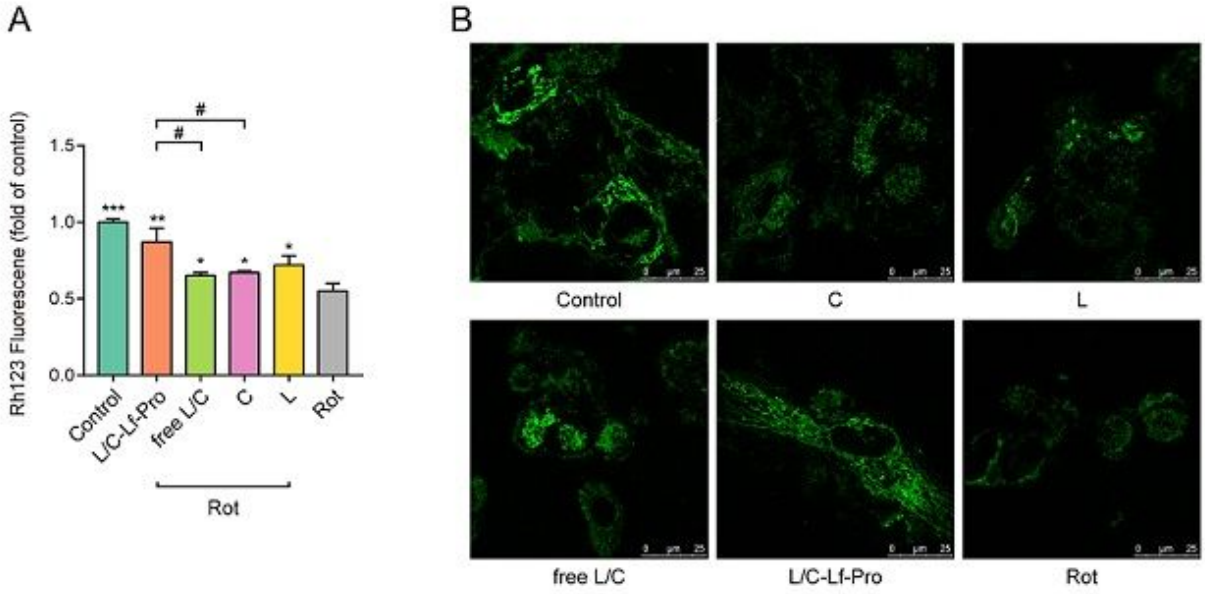

Figure 4

Lf-protocells suppressed Rot-induced mitochondrial dysfunction in SH-SY5Y cells. (A) Effect of lf-protocells on Rot-induced oxidative damage and mitochondrial dysfunction in SH-SY5Y cells. The mean fluorescence intensity of Rh123 was detected in each group. (B) The Rh123 accumulation in mitochondria was detected by confocal microscope (scale bar, 25 μm). (mean ± SD; n=3. * P < 0.05, ** P < 0.01, *** P < 0.001 compared with the 4 μM Rot group. # P < 0.05, compared between two groups.) Rot: rotenone; C: curcumin; L: levodopa; Lf-Pro: lf-protocells.

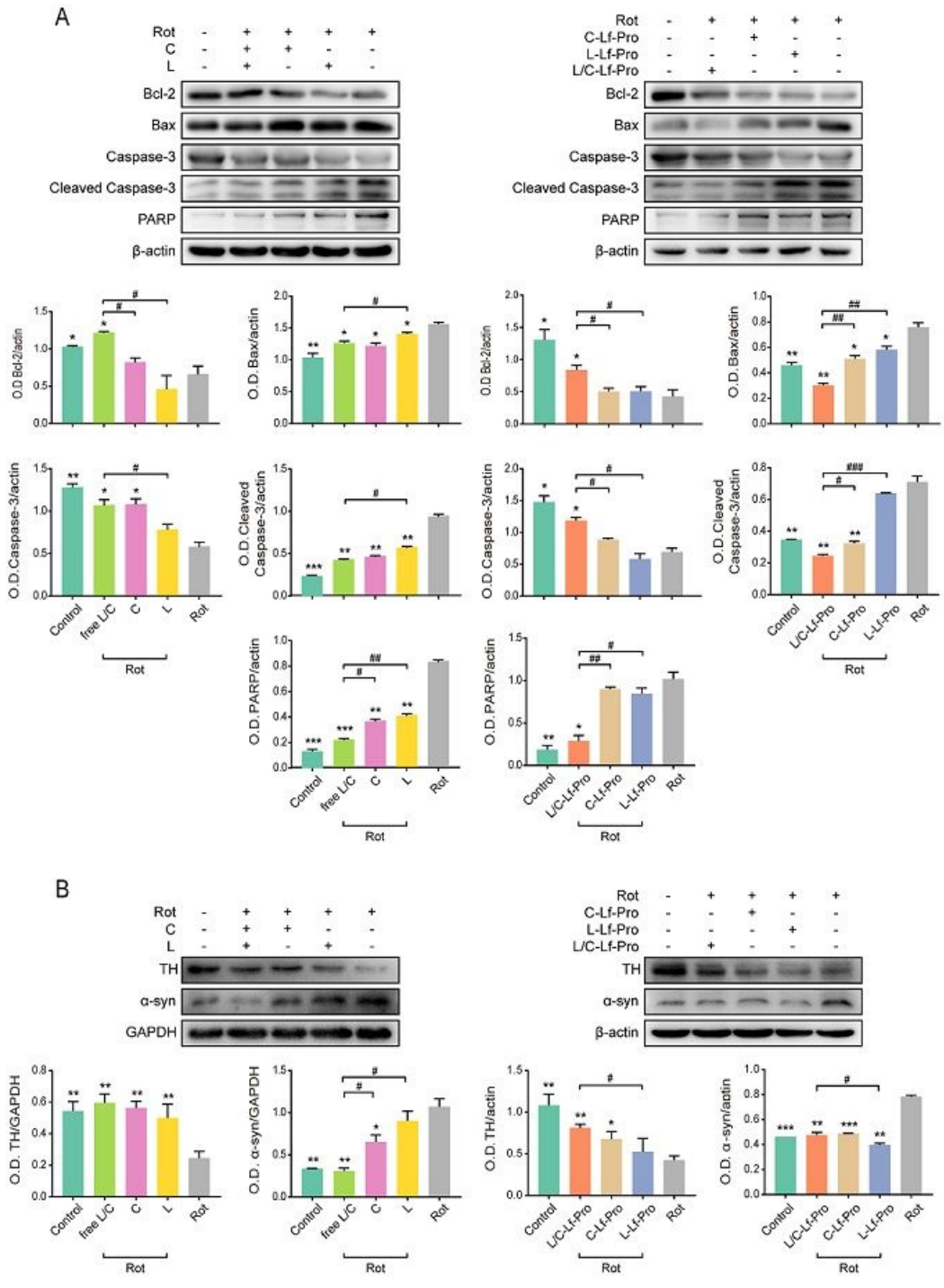

Figure 5

The effects of levodopa/curcumin and L/C-Lf-Pro on rotenone-induced variation in expression of apoptosis related proteins and PD related proteins through western blot analysis. Representative blots on the upper panels, along with bar graph summarizing group data on the bottom panels. (A) Expression of apoptosis related proteins in experimental groups. The expressions of Bax, Cleaved Caspase-3, PARP were decreased while the expressions of Bcl-2 and Caspase-3 were significantly increased by free L/C or L/C-Lf-Pro pretreatment compared with the 10 μM Rot group. Pretreatment with free L/C or L/C-Lf-Pro recovered the imbalanced expression profile of these proteins, protected SH-SY5Y cells against rotenone induced apoptosis. (B) Expression of PD related proteins in experimental groups. Pretreatment with free L/C or L/C-Lf-Pro reduced the accumulation of misfolded α-syn and enhanced the level of TH obviously compared with other groups. (mean ± SD; n=3. * P < 0.05, ** P < 0.01, *** P < 0.001 compared with the 10 μM Rot group. # P < 0.05, ## P < 0.01, ### P < 0.001 compared between two groups.) Rot: rotenone; C: curcumin; L: levodopa; Lf-Pro: lf-protocells.

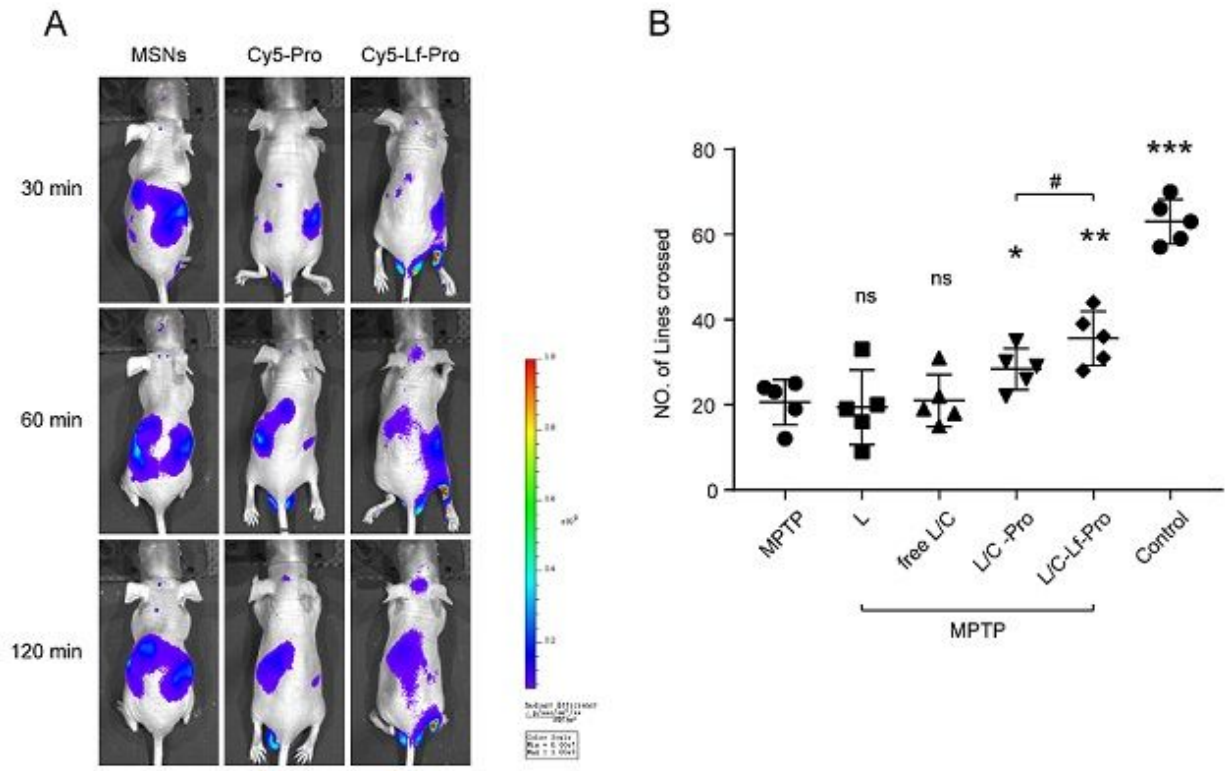

Figure 6

In vivo experiments on biodistribution and improvement of motor function deficits. (A) In vivo imaging of BALB/c-nu mice after administration of Cy5-MSNs, Cy5-protocells, Cy5-lf-protocells at 30, 60, 120 min. (B) Effects of L/C-Lf-Pro on locomotor function in MPTP-induced PD model mice. Sum of lines crossing in different experimental groups for five days. (mean ± SD; n=3. ns P > 0.05, * P < 0.05, ** P < 0.01, *** P <

0.001 compared with the MPTP group. # P < 0.05 compared between two groups.) Cy5-Pro: Cy5-potocells; Cy5-Lf-Pro: Cy5-lf protocells; Rot: rotenone; C: curcumin; L: levodopa; Lf-Pro: lf-protocells.

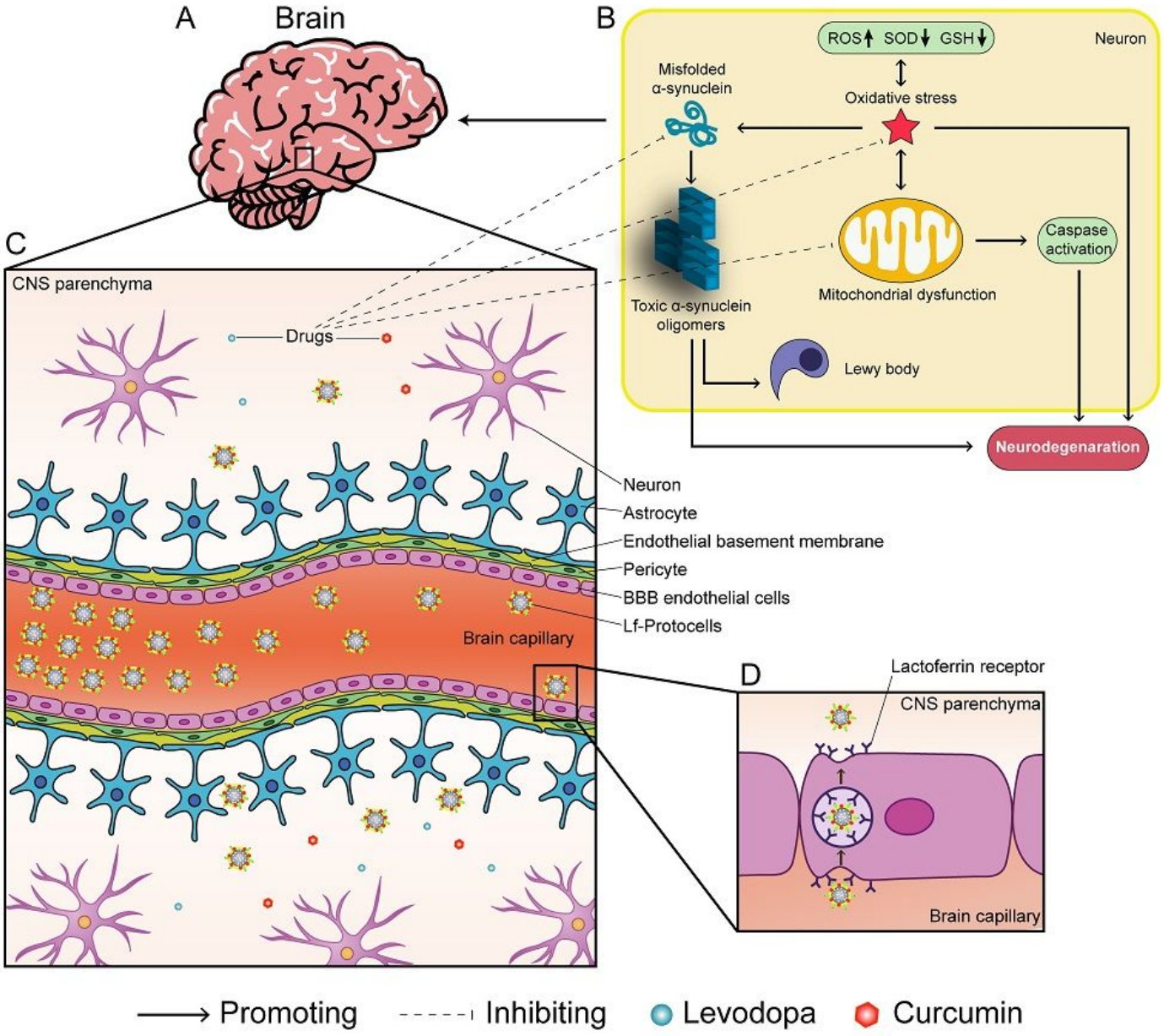

Figure 7

Schematic illustration of binary-drug loaded lf-protocells for treating Parkinson's disease. (A) Parkinson's disease (PD) is the second most frequent neurodegenerative disease. (B) The pathological hallmark of PD is the characteristic loss of dopaminergic neurons and the appearance of Lewy bodies formed by misfolded and oligomeric α-syn. Both mitochondrial dysfunction and oxidative stress are key elements in the pathogenesis of PD. (C) The blood-brain barrier (BBB) limits the delivery of the vast majority of drugs passing from the bloodstream into the brain. (D) Drug delivery system named as binary-drug loaded lf-protocells (L/C-Lf-Pro) shows greatly improved BBB transport efficiency of levodopa and curcumin through lactoferrin receptor-mediated endocytosis. While penetrating into the central nervous system,

levodopa and curcumin exhibit neuroprotective effects against PD with multiple mechanisms, including enhancing the cell viability, decreasing the expression of a-synuclein, ameliorating oxidative stress and mitochondrial dysfunction.

Supplementary Files

This is a list of supplementary files associated with this preprint. Click to download.

- supplementrevised.pdf